Band Parachutes in the Wake of Viking Entry Forebodies at Mach Numbers from 0.2 to 2.6," AEDC-TR-72-78, July 1972, ARO, Inc., Arnold Air Force Station, Tenn.

[10] "Propulsion Wind Tunnel Facility," *Test Facilities Handbook*, 9th ed., Vol. 4, Arnold Engineering Development Center, Tullahoma, Tenn., July 1971.

[11] "The Langley Transonic Dynamics Tunnel," Langley Working Paper LWP-799, Sept. 23, 1969, NASA.

[12] Steinberg, S. and Faye-Petersen, R., "Pre-Test Report for Flexible Decelerator Wind Tunnel Tests at AEDC PWT," TP-3720060, Jan. 1971, Martin Marietta Corp., Denver, Colo.

[13] Steinberg, S., "Pre-Test Report for Flexible Decelerator Wind Tunnel Tests at AEDC PWT 16T (Phase 2)," TP-3720157, June 1971, Martin Marietta Corp., Denver, Colo.

[14] Jaremenko, I., "Pre-Test Report for Flexible Decelerator Wind Tunnel Tests at AEDC PWT 16S," TP-3720168, July 1971, Martin Marietta Corp., Denver, Colo.

[15] Moog, R. D. and Michel, F. C., "Balloon Launched Viking Decelerator Test Program Summary Report," TR-3720359, March 1973, Martin Marietta Corp., Denver, Colo.

[16] Dickinson, D., Schlemmer, J. W., Hicks, F., Michel, F. C., and Moog, R. D., "Balloon Launched Decelerator Test Program; Post-Flight Test Report, BLDT Vehicle AV-4," TR-3720295, Oct. 1972, Martin Marietta Corp., Denver, Colo.

FEBRUARY 1974 J. SPACECRAFT VOL. 11, NO. 2

Skylab Experience with Apollo Docking/Latching Loads

R. A. HEATH*
Martin Marietta Aerospace, Denver Division
AND
W. B. HOLLAND†
NASA Marshall Space Flight Center, Huntsville, Ala.

Since the early development stages of Apollo, the docking probe mechanism has confronted the structural dynamicist with a modeling and structural response challenge. Skylab is an excellent example of a structure where complexity of analytical models and subsequent dynamic analysis is fully justified. This paper describes the four-year development of Skylab analytical programs, mathematical model complexity, and vibration and load analyses associated with the docking/latching maneuver. Examples are shown where coarse models produced loads in excess of structural capability. However, subsequent model refinement lowered the loads to the point where redesign was not required. A summary of experience gained over a four-year period is presented in the conclusions.

I. Introduction

SKYLAB is a 100-ton manned orbital scientific space station designed to accomplish scientific and technical experiments and medical investigations while in near-earth orbit. The primary source of power for Skylab is provided by large flexible solar array systems (SAS) which require special handling to prevent panel buckling or other structural damage under their own weight.

The transient loading conditions, occurring during the atmospheric boost phase of flight, design the primary structural elements of Skylab with the exception of the docking interfaces, solar arrays, and deployment structure. The orbital vacuum environment causes no external forces on the vehicle. The orbital events considered in the design of Skylab are docking, latching, orbit maneuvers, and the several deployment sequences. Since docking and latching are the significant load-producing events, this paper will be limited to the discussion of these two events.

In the early design stages of Skylab, an acceleration value of 0.2 g was used to simulate the loads due to the orbital docking and latching event. This was adequate for preliminary design, but changed considerably as the design progressed. Docking and latching forcing functions were derived and used to calculate the response loads at selected coordinates. This process became more complicated as the models grew in sophistication.

This paper describes the evolution of the Skylab models and the vibration analyses performed in support of the docking and latching event. In addition, the paper lists criteria derived from Skylab experience and considered applicable for future orbital space station development.

II. Configurations

The Skylab orbital cluster consists of the Orbital Workshop (OWS), Instrument Unit (IU), Fixed Airlock Shroud (FAS), Airlock Module (AM), Structural Transition Section (STS), DA truss, Multiple Docking Adapter (MDA), deployed ATM, and deployed SASs of the ATM and OWS. When the Command and Service Module (CSM) docks to the axial port of the MDA, this configuration (Fig. 1) is called Axial Configuration. The rescue mission requires the use of another CSM docked to the MDA radial port; this is referred to as Radial Configuration. These are the configurations used to perform the vibration and loads analyses which follow.

III. Skylab Vibration Analyses Chronology

In early 1969, mathematical models were represented primarily with equivalent beam stiffnesses. This "stick" model consisted of a mass spring representation of the modules which make up the configuration of Fig. 1. Only the ATM rack structural model is

Presented as Paper 73-613 at the AIAA/ASME/SAE Joint Space Mission Planning and Execution Meeting, Denver, Colo., July 10–12, 1973; submitted July 20, 1973; revision received October 1, 1973.

Index category: Structural Dynamic Analysis.

* Group Engineer—Skylab Dynamics. Member AIAA.

† Dynamics Engineer.

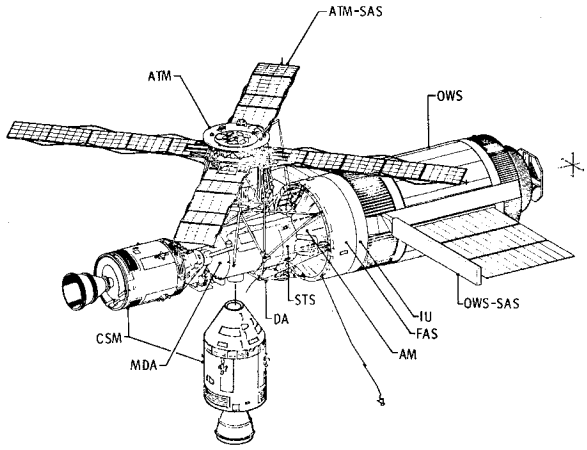

Fig. 1 Skylab docking configurations.

a finite element representation of the stiffness of the actual structure. The formulation of such a model involves the idealization of an actual structural member or assembly of members into a series of discrete or finite elements. These elements are considered to be connected at node points to form a network or model from which stiffness characteristics may be obtained for the structure, using a digital computer program. The Martin Marietta system of structural analysis programs utilizes the direct stiffness method. A stiffness matrix is formed for each discrete element (axial member, beam, plate, etc.) and the element stiffness matrices are merged to form the over-all stiffness matrix for the entire assembly represented by the model. To obtain good representative stiffness characteristics of a complex structure, the original model is formed in more detail than that used in the dynamic model. The large stiffness matrix is then reduced or collapsed to one of more manageable proportions. The effect of all intermediate, or collapsed, stiffnesses is still retained in the final stiffness matrix.

The technique used to compute the modes is modal coupling,[1] with the modes of the various components being computed separately. These uncoupled modes are mathematically coupled and transformed to form a set of coupled modes. During this coupling process, a frequency cutoff criterion is defined for the coupled mode set. The frequency limit then determines the number of component modes required in the coupled analysis. The total degrees of freedom (DOF) which make up this model, prior to any reduction, will approach 20,000 DOF.

It is known that some component modes are more important than others in modal coupling. The obvious place to look for the important component modes is in the ATM and OWS solar arrays, since these two components account for approximately 80% of the total number of modes required. The method for selecting the important component modes involves selecting the solar array modes which have the largest effect on the main beam response and discarding all others in the vibration analysis.[2] To calculate accurate loads on the solar arrays, all panel modes must be used. The method employed was to calculate the accelerations at the solar panel attachment point on the model with the truncated panel modes and to use the accelerations to base drive the solar array cantilevered modes.

In 1971, it was recognized that the vibration analyses used for the loads analyses are not necessarily sufficient for control system analyses. The concept of uniform frequency cutoff was used for the controls model. This concept is to retain all modes of each component to a specific frequency determined by the size limitation of the computer program, which at this time was 115 DOF. The modal selection technique does not guarantee maximum control moment gyro (CMG) or rate gyro motion. Of course, this limited the frequency definition in the controls model to slightly less than 5.0 cps. As one might suspect, this is not an adequate model for loads calculations. Here again, the modal selection technique was employed to increase the frequency definition of the loads model above 10 cps.

In 1972, the decision was made to assess the accuracy of the loads vs the controls modes, to assess the validity of solar array modal selection techniques, and to determine an acceptable frequency fidelity for vibration analyses. It was concluded that all future vibration analyses will contain individual component frequencies equal to or greater than 15.0 cps. The solar arrays will use consecutive uncoupled modes up to 5.0 cps and use modal selection technique for defining important modes up to 15.0 cps. A single model for both loads and controls analysis, determined in accordance with the aforementioned criteria, is considered more accurate than previous vibration analyses based on consecutive modes and frequency cutoff for a limited number of coupled modes. The mathematical models are now so complex that the final modal coupling run using over 200 DOF requires a CDC 350K core storage capacity.

Another interesting learning experience has come to the surface in the field of mathematical modeling. The Skylab models are developed from approximately 11 modules. In the modal coupling procedure, several modules are tied together to form a main beam. The remaining modules are modally coupled to the main beam. For this example, the main beam consists of the FAS, IU, and OWS modules. The finite element models for these structures are developed by NASA associate contractors. Historically, interface loads have been required at the FAS/IU and IU/OWS, which makes it desirable to have a centerline point at each of these interfaces. There is a limitation to the number of degrees of freedom which can be retained in a dynamics model. Another reason to maintain a centerline node point is to make the main beam module compatible with the sizes of the other modules. However, the centerline coordinates were not modeled in the original model. To derive a centerline node point, the radial degrees of freedom were first reduced out to allow radial motion to occur in a typical breathing mode manner. A geometric transformation relating IU ring motion of all tangential and longitudinal coordinates in terms of motion at the IU centerline reduces further the number of IU ring interface coordinates. Coupling which occurs between the radial and tangential degrees of freedom in effect constrained the IU ring motion radially. A visual analogy of this phenomenon is to imagine that the IU centerline point represents the motion of a radially slotted rigid plate. This caused the OWS-SAS loads to be conservative to the point of exceeding published design limits. In order to alleviate this situation, all IU coordinates are collapsed out of the main beam model. This allows the main beam stiffness model to reflect the OWS-SAS attach point

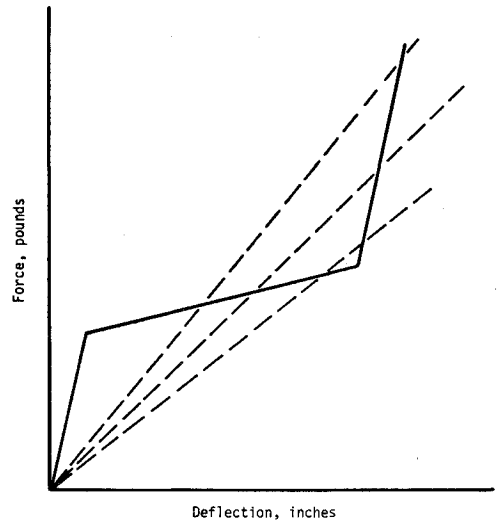

Fig. 2 Nonlinear force deflection relationship.

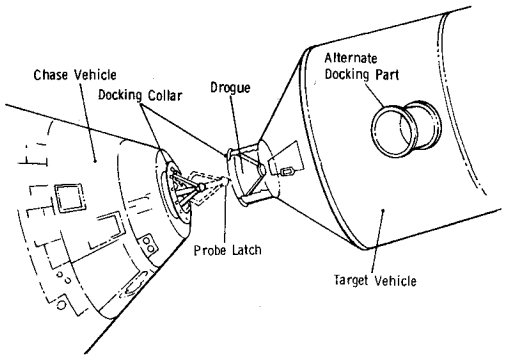

Fig. 3 Docking maneuver.

flexibility as defined in the original IU finite element model, thus alleviating the problem with the OWS-SAS loads.

A facet of modeling which had to be considered on Skylab was providing an adequate vibration analysis where it was known that a component of the configuration exhibits nonlinear behavior. This was true particularly in the ATM where the gimbal ring assembly (GRA) is suspended within the rack on a nonlinear spring. The spring rate is high for small deflections up to the point where the preload in the spring is relieved and becomes soft thereafter, until the GRA bottoms out on the rack stop. A simple illustration of this problem is demonstrated with the load-deflection curve of Fig. 2. For a control system vibration analysis, where vehicle forces are small, it is reasonable to use a GRA spring constant based on the force deflection range which passes through the origin of Fig. 2. The docking and latching forcing functions cause GRA responses and corresponding deflections which operate in the nonlinear range of Fig. 2. The cost and schedule impact of performing a nonlinear analysis dictated the use of an iterative process in the vibration analysis using the spring constants and frequencies determined from the dashed lines of Fig. 2. Luckily, a few iterations of the GRA frequency produced a model which provided loads consistent with the desired force-deflection relationship.

IV. Docking/Latching Maneuver

The docking/latching loads analysis is a two-step operation consisting of the forcing function computation and the determination of loads at selected coordinate interfaces due to the forcing functions. If the computer capacity were large enough, it would be possible to calculate the forcing function and the response thereto in a single operation. Since this is not possible, it is necessary to separate the forcing function program from the response program.

The maneuver simulated by the docking/latching program consists of the following events:

1) The CSM docking probe impacts the MDA drogue at predetermined velocities and orientations.
2) Subsequent to the sliding and bouncing motion of the docking probe against the drogue, the probe head is captured in the apex of the drogue cone and secured by the three capture latches.
3) If the manual retract mode is selected, the CSM is aligned with the MDA by manual firing of the CSM control thrusters and, after the desired aligment is achieved and all relative rates have subsided, the probe is retracted, drawing the docking rings together. For simulation, the relative rates are assumed to be zero and the misalignment angle measured between the docking rings is assumed to be 3°.
4) If the automatic retract mode is selected, the probe begins retract 0.15 sec after probe head capture and before the docking impact transients have diminished, thus producing a much more severe condition than the manual retract mode. It should be emphasized that the manual retract mode is the nominal mode and that under the current operating procedure, automatic retract can occur only due to a pilot error.
5) Regardless of which retract mode is simulated, the 12 docking latches are activated individually when the docking ring misalignment angle is 3° or less, and when their respective triggers are tripped as the docking rings close to within 0.105 inch. There is a 0.028-sec time delay associated with each automatic latch sequence required for the latch to deploy and make contact with the CSM docking ring.
6) After the 12 latches have triggered and the CSM has become "hard latched" to the MDA, the simulation is continued for approximately 10 sec, until docking transients are damped out.

The Apollo docking mechanism is a relatively complex mechanism consisting of a probe assembly mounted on the CM and a drogue assembly mounted on the MDA (Fig. 3). The primary component of the docking probe assembly is the probe body, consisting of an inner cylinder that moves axially with respect to an outer cylinder (Fig. 4). The probe barrel is structurally fastened to the CM by a support consisting of three symmetrically oriented strut/beam assemblies (tripod mount). A conical probe head is swivel mounted to the end of the inner cylinder. Additionally, the docking probe assembly has three symmetrically-oriented pitch arm assemblies, each consisting of a tension link, shock attenuator, and a pitch arm. The drogue assembly is a conical structure that is truncated to provide a receptacle for the probe head in the captured position.

The docking analysis considers the two vehicles to be in relative proximity initially (Fig. 3). During the maneuver the probe head and one or more of the three pitch arms may engage in sliding contact with the drogue. The initial coupling of the two vehicles is achieved when the probe head is seated in the receptacle and three symmetrically-located probe head latches secure the probe head to the drogue. This effectively creates a hinged joint between the two vehicles; the pitch arms serve to prevent jack-knifing.

After the probe head has been successfully secured to the drogue, retraction of the probe assembly may occur. During retraction, the probe assembly foreshortens (due to high-pressure gas acting on a piston on the end of the inner cylinder) and draws the vehicles close. The pitch arms "flare" out to cause less and less clearance between the arms and the outer lip of the drogue, resulting in a positive attitude alignment.

After the probe assembly has fully retracted, the docking collars (Fig. 3) are close enough that latches situated on the probe side of the docking interface (on the docking collar) secure the two mating rings or collars in a final hard structural connection.

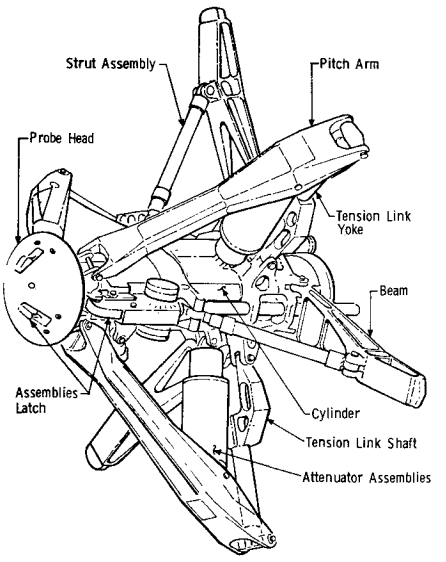

Fig. 4 Apollo docking probe assembly.

The docking/latching digital simulation program is documented in great detail in Ref. 3. The following paragraphs summarize the significant features of the program without mathematical detail.

The docking/latching simulation program consists of a number of FORTRAN subroutines which simulate the docking of two elastic space vehicles (the CSM and the Skylab cluster) by use of the Apollo docking mechanism. Included in these subroutines are those which simulate the three control systems, Thrust Augmented Control System (TACS), Control Moment Gyros (CMG), Reaction Control System (RCS). The control system subroutines compute control torques which attempt to damp out rate and attitude transients due to docking impact.

Basically, the simulation program requires as input data such things as mass and inertia data of the two vehicles, probe geometry, probe stiffness and damping characteristics, initial relative orientations and rates of the two vehicles, and some number of elastic modes for a specific Skylab configuration. The number of elastic modes required to define an accurate forcing function is covered later in this paper.

Using the above information, a state vector containing the necessary velocities, forces, and positions to describe completely the state of the system is defined. This state vector is then integrated using a fourth-order Runge-Kutta-Gill numerical integration scheme. The simulation thus proceeds through all or any sequential portion of the docking, retract, latching, and post-latching procedure necessary to secure the CSM to either the axial or radial docking port of the Skylab cluster.

V. Docking Forcing Functions

In the early design stages of Skylab, it was decided by NASA that the ground rules for the docking analysis should use the same design criteria as established for Apollo-LM docking. Table 1 lists the CSM probe head miss distance and angular misalignment, CSM closing velocity and CSM-RCS thrust values. Of the countless combinations of initial conditions that might be considered, 18 axial and 18 radial docking cases were considered adequate to envelope the docking loads. This included both a straight-in and undocking case.

When the docking/latching program was first developed, it was considered adequate and economical to limit the program to accepting 26 elastic body modes. In order to evaluate the adequacy of 26 modes, a transfer function analysis relating docking port deflections and rotations to docking port forces and moments is calculated at both the axial and radial ports

Table 1 Docking program

Criteria		
Alignment	Radial	± 12 in.
	Angular	$\pm 10°$
Velocities	Axial	1.0 fps
	Radial	0.5 fps
	Angular	1.0°/sec
Thrust	400 lb (CSM-RCS)	
	Time-Probe head contact to 0.4 sec after probe head capture	
Conditions	18 combinations of above per configuration	
Math model	CSM—6 DOF	
	Cluster-6 DOF plus $\leqq 26$ elastic modes $\leqq 6$ cps and show significant amplitude at docking port	
	Probe mechanism—nonlinear effects of	
	1) Damping characteristics of three shock attenuators	
	2) Force—deflection characteristics of deformable parts	
	3) Large geometry changes caused by deformation	
Forcing functions $F(x, y, z)$ and $M(x, y, z)$ at CSM/MDA I/F		

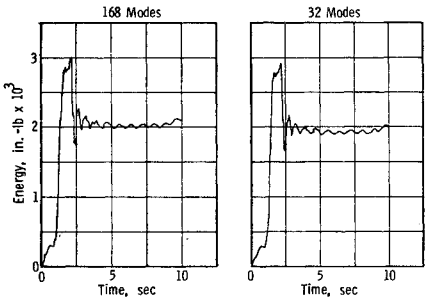

Fig. 5 Axial docking AZAIO energy plots.

(Fig. 1) for the configuration of interest. The modes which show the largest docking port participation are selected from the total number of coupled modes required to provide a 15.0 cps mathematical model. The transfer functions are recalculated using only the selected modes. A comparison of the two sets of data confirms that the selected modes reproduce the transfer functions of the case using all available modes. This could be misleading if the response at other vehicle stations happens to be in a frequency domain other than that represented by the 26 selected modes. In order to preclude this possibility, it was deemed necessary to calculate the energy transferred from the CSM to the cluster using all available system modes versus the selected modes used to calculate the forcing function.

The energy evaluation consisted of using the following relationship

$$\{q\}^T[\phi]^T([M][\phi]\{\ddot{q}\}+[C][\phi]\{\dot{q}\}+[K][\phi]\{q\}) = \{q\}^T[\phi]^T\{F\}$$

where $\{q\}$ = generalized displacement matrix; $[\phi]$ = modal displacement matrix; $[M]$ = discrete mass matrix; $[C]$ = discrete damping matrix; $[K]$ = discrete stiffness matrix; and $\{F\}$ = applied forcing function.

The exact solution could only be achieved by calculating the forcing function and the vehicle response using all the modes, i.e., model frequency definition up to 15.0 cps. Since this quadruples the cost of computing a forcing function, it was desirable to see how adequately the forcing function generated by 26 elastic body modes duplicated the energy transferred from the CSM to the cluster. All docking forcing functions $\{F\}$ are calculated using the selected 26 elastic body modes. The comparison of energy between using all the modes versus the case using 6 rigid body plus 26 elastic body modes is presented in Table 2. Energy buildup histories are presented in Fig. 5 for axial docking case AZAIO to illustrate how 168 modes used in

Table 2 Docking program energy comparison

Docking condition[a]	No. of modes	Energy (in.-lb)	No. of modes	Energy (in.-lb)	Energy (%)
Axial AZAIO	168	3023	32	2936	97.2
Axial AZTOO	168	2440	32	2381	97.5
Axial AYTIO	168	2834	32	2508	88.6
Radial RXAII	173	4797	32	4771	99.5
Radial RXAIO	173	3086	32	3066	99.3
Radial RYAIO	173	3486	32	3408	97.8

[a] Nomenclature represents a combination of initial conditions from Table 1 and are further defined in Ref. 4.

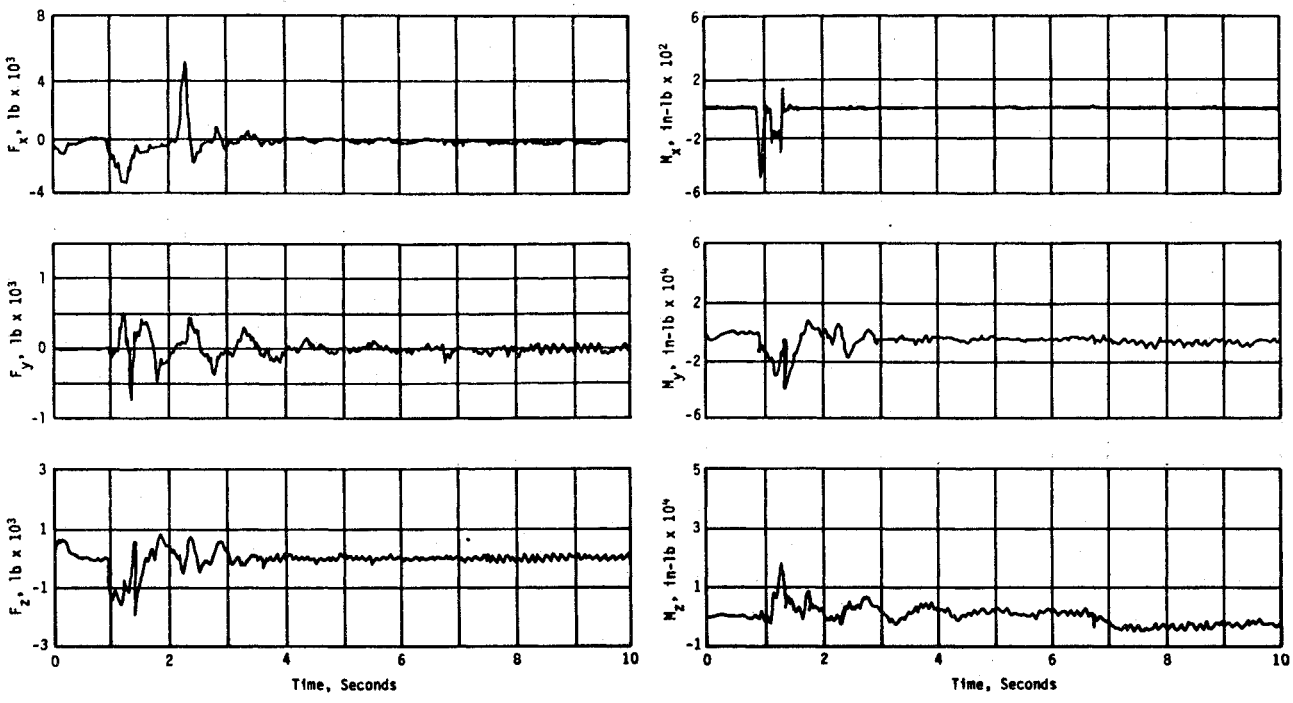

Fig. 6 Axial docking AZAIO forcing function.

the computation of energy compare with 32 modes. It is concluded that the selected modes are adequate to produce cluster response up to the frequency limitation of the mathematical model.

A typical axial port docking forcing function is presented in Fig. 6. The docking forcing functions consist of three forces and moments referenced to the CSM/MDA docking port centerline, three CMG moments and six individual TACS thruster forces. Only the docking port forces are presented since these are the significant forces with respect to determining cluster dynamic response. Even so, the probe and pitch arm impact loads are small with respect to the loads developed during latching.

VI. Latching Forcing Functions

The latching model is an excellent example where complexity of the model and subsequent dynamic analysis is fully justified. Early in the Skylab program, latching was simulated with rigid chase and rigid target vehicles connected by a flexible interface. Both vehicles were free to move with 6 DOF and no probe stiffness was considered. The automatic latches, represented by a linear spring, transferred axial load only with no shear, or torsion capability. The results of this analysis showed that latch loads and CSM/MDA bending moments exceeded the limit design values of the latch and axial port. These values were known to be conservative since the only flexibility in the system was introduced through the latches. This made it necessary to simulate the docking/latching maneuver more adequately, including vehicle elastic body modes. In addition, latching analysis was revised to use the individual latch force-deflection curve of Fig. 7. Whenever the latches separate, the 56,600 lb/in. portion of the curve is followed. Nineteen axial and 22 radial latching cases were calculated to establish the envelope of docking port maximum bending moments of Fig. 8. These cases reflect probe retract initiated at the various orientation angles of the 12 latches. The modal selection technique for latching is the same as that used in the docking program. The latching forcing functions comprise three forces and moments referenced to the CSM/MDA centerline, three CMG moments, and six individual TACS thruster forces. Only the docking port forces are significant with respect to determining cluster dynamic response.

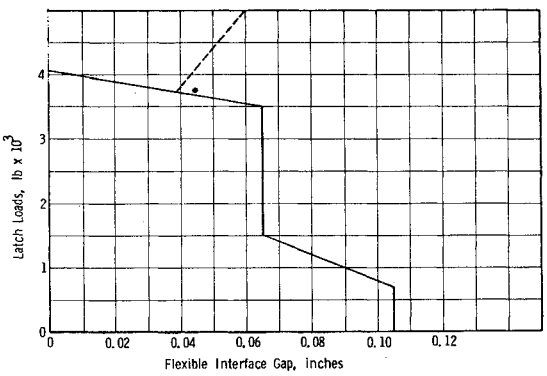

Fig. 7 Latch force deflection.

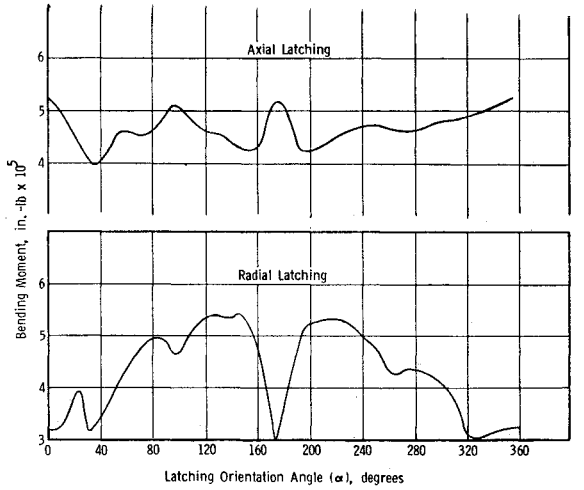

Fig. 8 Latching CSM/MDA interface moment.

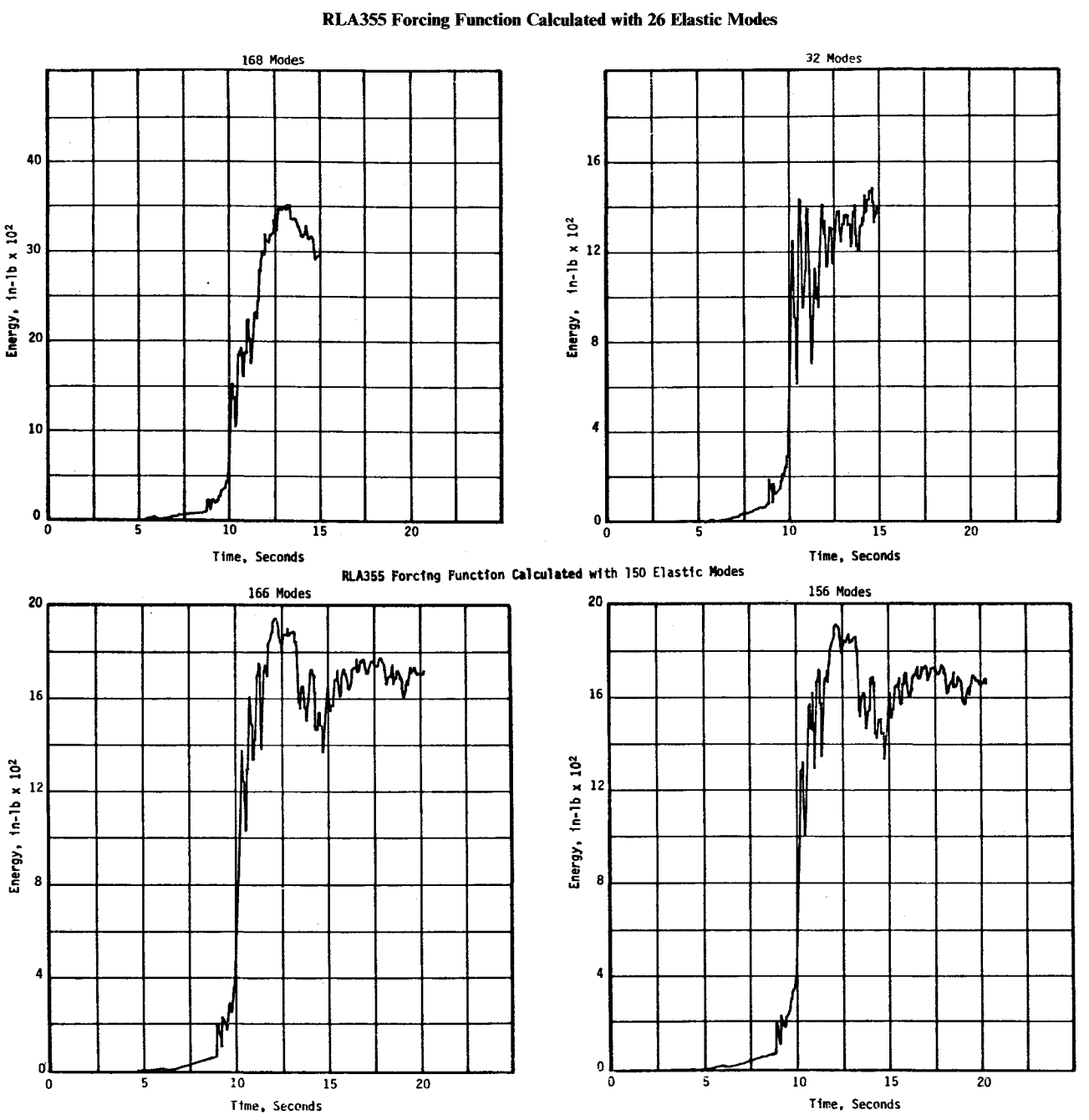

Fig. 9 Axial latching RLA355 energy plots.

It was seen that when a major load-contributing mode to a solar array is omitted in the computation of the forcing function and then loads on the solar array are determined with the omitted mode included in the base-driven response calculation, it is possible to cause a near-resonant excitation in that mode. This led to the suspicion that docking port loads were sensitive to the number of elastic body modes used in the docking/latching program. In an effort to achieve a quick resolution to the sensitivity of the latching forcing function, it was decided to choose 25 modes from the axial configuration, filling in the modes around 1.3 cps and omitting some of the other modes, because the first two bending modes of the cluster axial configuration are 1.28 and 1.39 cps. Experience has shown that the latching forcing functions can be approximated by motion of the CSM rocking on the docking port at the Skylab natural frequency. Table 3 presents the frequency comparison between the 26 and 25 selected mode cases from the final vibration analysis. It might be anticipated that the latching forcing functions from either set of modes would be similar in magnitude and frequency content. Table 4 shows that they are not, which made it apparent that an evaluation of energy transferred from the CSM to the Skylab was in order. To expedite this calculation, the restriction of accepting 26 elastic body modes was eliminated by increasing the number of modes to 150.

The methodology for evaluation of energy transferred is defined in the preceding section. If the energy transferred from the CSM is reasonably close to the energy developed in the response program, it should be concluded that sufficient modes are used to develop an adequate latching forcing function. Table 5 shows the energy comparison for the RLA355 forcing function, varying the number of Skylab elastic body modes. The latching forcing functions are supplied to the response program, where the energy is recalculated using all modes and the specific number of modes used to generate the forcing function. It is obvious from Table 5 that only the latching forcing function using all modes yields energy values which show compatibility

Table 3 Selected modes for docking/latching

No.	26 selected modes		25 selected modes	
	Mode No.	Frequency (cps)	Mode No.	Frequency (cps)
1	7	0.183	9	0.187
2	8	0.183	10	0.188
3	9	0.187	11	0.378
4	10	0.188	12	0.387
5	11	0.378	13	0.444
6	12	0.387	14	0.445
7	13	0.444	17	0.500
8	14	0.445	18	0.509
9	17	0.500	19	0.554
10	18	0.509	20	0.557
11	19	0.554	23	0.608
12	20	0.557	37	0.910
13	23	0.608	38	1.043
14	39	1.158	39	1.158
15	40	1.250	40	1.250
16	41	1.282	41	1.282
17	46	1.348	42	1.312
18	47	1.961	43	1.335
19	69	3.038	44	1.337
20	93	5.468	45	1.346
21	94	5.535	46	1.348
22	95	5.772	47	1.961
23	96	5.908	93	5.468
24	97	6.092	94	5.535
25	102	6.124	95	5.772
26	103	6.145		

Table 4 Maximum docking port axial latching loads, RLA355

No. of modes	Damping value	Freq. (cps)	F_{Axial} (lb)	F_{RSS} (lb)	M_{RSS} (in.-lb)	Latch load (lb)
26	0.01	Table 3	7734	4015	524239	4931
25	0.01	Table 3	7744	3420	542270	5232
25	0.016	Table 3	8000	3469	529794	5211
63	0.016	3.038[a]	7026	4163	532383	5033
150	0.016	13.013[a]	6950	4399	471218	4623

[a] Consecutive modes up to frequency shown.

with the response program results. It is concluded that latching forcing functions should be calculated using all elastic body modes. The energy-time history plots for latching case RLA355, comparing the first and last case presented in Table 5, are shown in Fig. 9 to illustrate the necessity of using sufficient modes to achieve an energy balance between the forcing function and response programs. The latching forcing functions for these same two cases are presented in Fig. 10. The computer time required to calculate a latching forcing function is increased by a factor of four due to inclusion of the additional modes.

VII. Skylab Loads

An interesting example of when coarse models produced loads in excess of structural capability became apparent in the final loads analysis. It was found that the mathematical model was

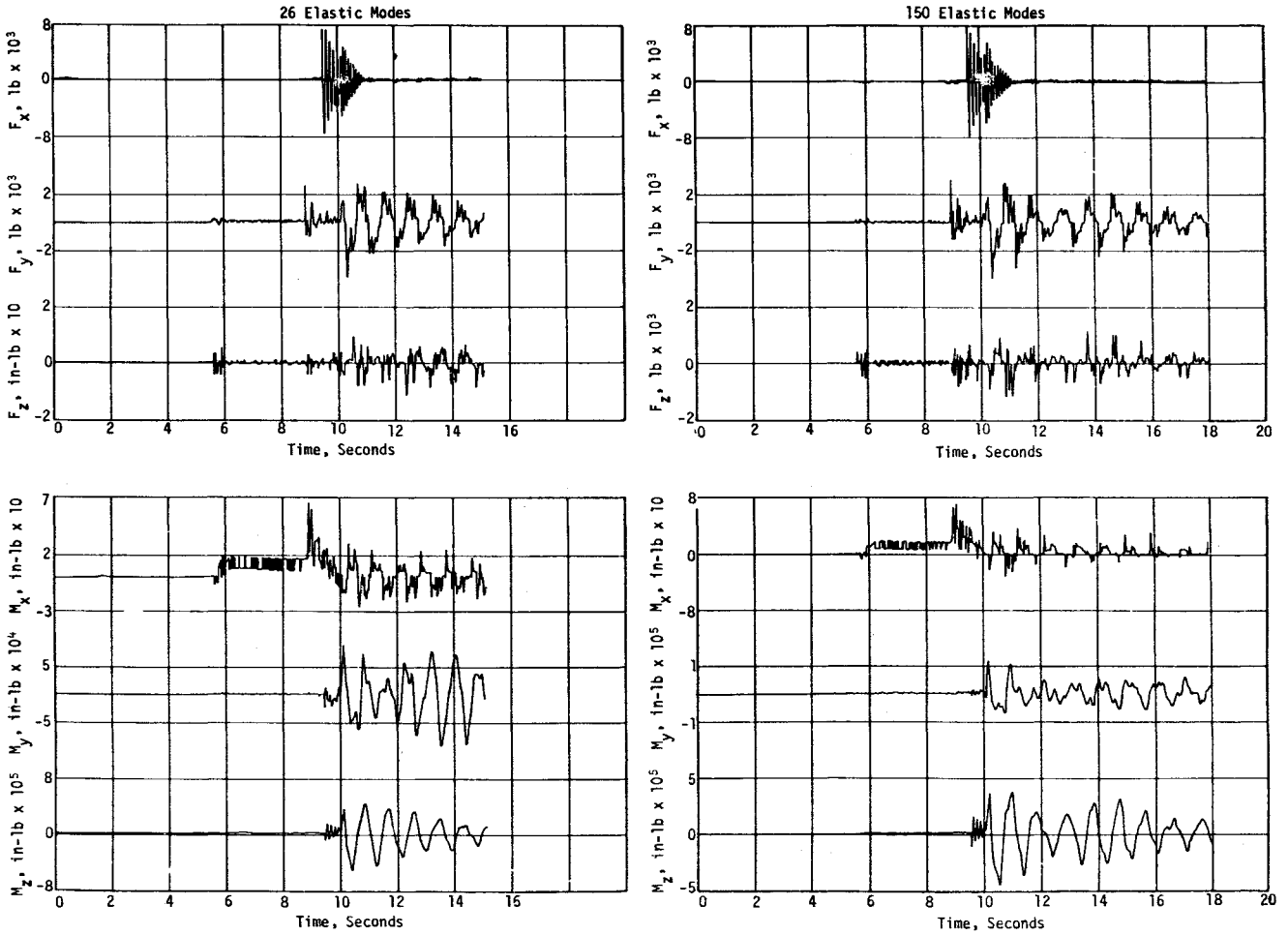

Fig. 10 Axial latching RLA355 forcing function.

Table 5 Latching program energy comparison

Forcing function program					Response program				
Configuration	Condition[a]	No. of elastic modes	Frequency (cps)	Energy (in.-lb)	No. of modes	Energy (in.-lb)	No. of modes	Energy (in.-lb)	Damping
Axial	RLA355	26	Table 3	[b]	168	3513	32	1471	0.010
Axial	RLA355	25	Table 3	[b]	168	4346	31	1967	0.010
Axial	RLA355	25	Table 3	[b]	168	4590	31	2004	0.016
Axial	RLA355	63	3.038[c]	1906	168	6105	69	1910	0.016
Axial	RLA355	150	13.013[c]	1920	168	1995	156	1971	0.016
Axial[d]	RLA000	150	13.366[c]	2000	166	1890	156	1836	0.010
Axial[d]	RLA098	150	13.366[c]	2060	166	1930	156	1911	0.010
Axial[d]	RLA194	150	13.366[c]	1920	166	1929	156	1912	0.010
Axial[d]	RLA355	150	13.366[c]	2070	166	1945	156	1911	0.010

[a] Retract is initiated with 3° misalignment.
[b] Data not calculated.
[c] Consecutive modes up to frequency shown.
[d] Updated vibration analysis with model deficiencies corrected.

crudely represented in the OWS-SAS attachment and the spar-canister/gimbal ring assembly. This required a supplemental vibration and loads analysis to resolve this issue. The mathematical model was found to be deficient in the definition of the orbital lock springs and the axial and radial roller springs. The FAS/IU/OWS forward skirt had additional constraints due to the manner in which the main beam component was formed, thus causing the OWS-SAS loads to be overconservative. This particular modeling problem was addressed earlier in this paper.

The latching forcing functions were recalculated using 150 consecutive elastic body modes in lieu of the original 26 selected modes. As an example of the conservatism caused by both modeling and forcing function inadequacies, the OWS-SAS beam fairing M_x bending moment was reduced from 152,000 in.-lb to 101,000 in.-lb, the orbital locks loads were reduced from 3347 lb to 1458 lb, and the flexible actuator axial load was reduced from 3140 lb to 1542 lb. In conclusion, the more sophisticated analysis indicated loads within the strength capability of the structure.

VIII. Conclusions

The vibration analysis for a structure such as Skylab should contain a frequency definition which includes all the fundamental modes of the uncoupled structure prior to implementing the modal coupling technique. The modal selection technique provides a tool for selecting important solar array elastic modes and eliminating others to increase the frequency fidelity of the mathematical model. Even so, it is recommended that all solar array modes within the frequency realm of the control system be included in the vibration analysis.

Care should be exercised in modeling the juncture of beam and finite element stiffness properties in order not to constrain the expected motion artificially. This may cause apparent load problems where none exist.

A model which contains a module exhibiting nonlinear behavior may require an iterative vibration analysis to approximate a compatible linear system.

A transfer function analysis to select the number of elastic body modes required to calculate an adequate forcing function may be misleading if the cluster response happens to be in a frequency domain other than that represented in the selected modes. An energy evaluation approach, comparing the energy transferred from the CSM orbital cluster between the forcing function program and the response program, provides a better method for predicting the adequacy of the forcing function. Coarse models tend to produce conservative loads whereas sophisticated models account for more vehicle flexibility and hence more realistic loads.

References

[1] Benfield, W. A. and Hruda, R. F., "Vibration Analysis of Structures by Component Mode Substitution," *AIAA Journal*, Vol. 9, No. 7, July 1971, pp. 1255–1261.

[2] Morosow, G. and Abbott, P., "Mode Selection," ASME 1971 Winter Annual Meeting, Nov. 1971.

[3] Bodley, C. S. and Park, A. C., "Skylab Docking Maneuver Simulation Mathematical Model Report (Final)," TR ED-2002-1395, Contract NAS8-24000, Nov. 1971, Martin Marietta Corp., Denver, Colo.

[4] Uchiyama, J. T. and Heath, R. A., "Skylab Cluster Docking/Latching Loads Report (Final)," TR 10M3115, Contract NAS8-24000, March 1973, NASA.